

Laser metrology for ultra-stable space-based coronagraphs

Joel A. Nissen*, Alireza Azizi, Feng Zhao, Shannon Kian G. Zareh, Shanti R. Rao, Jeffrey B. Jewell, Dustin Moore

Jet Propulsion Lab 4800 Oak Grove Dr, Pasadena, CA 91109 (USA)

ABSTRACT

Sensing starlight rejected from a coronagraph is essential in stabilizing the telescope pointing and wavefront drift, but performance is degraded for dim stars. Laser Metrology (MET) provides a different, complementary sensing method, one that can be used to measure changes in the alignment of the optics at high bandwidth, independent of the magnitude of the host star. Laser metrology measures changes in the separation of optical fiducial pairs, which can be separated by many meters. The principle of operations is similar to the laser metrology system used in LISA-Pathfinder to measure the in-orbit displacement between two test masses to a precision of ~ 10 picometers. In closed loop with actuators, MET actively maintains rigid body alignment of the front-end optics, thereby eliminating the dominant source of wavefront drift. In the case of a segmented, active primary mirror, MET provides six degrees of freedom sensing, replacing edge sensors. MET maintains wavefront control even during attitude maneuvers, such as slews between target stars, thereby avoiding the need to repeat time-consuming speckle suppression. These features can significantly improve the performance and observational efficiency of future large-aperture space telescopes equipped with internal coronagraphs. We evaluate MET trusses for various proposed monolithic and segmented space-based coronagraphs and present the performance requirements necessary to maintain contrast drift below 10^{-11} .

Keywords: Laser Metrology Coronagraph

1. INTRODUCTION

Stellar coronagraphs work by focusing the light from a star onto a mask, which acts to suppress the starlight at the center of the field while allowing transmission of light from nearby planets. Coronagraphs use “speckle suppression” image-based wavefront sensing and deformable mirrors to tune a “dark hole” around the host star, creating a high-contrast region for planet detection and characterization. Speckle-suppression sensing is an iterative process that relies on long integration times to collect photons from the residual starlight suppressed by a factor of 10^9 or more. It is essential that the wavefront is stable for long periods of time or the speckle suppression technique will not converge. It is expected that future space-based coronagraphs will require contrast stability of 10^{-11} at the IWA for hours to days and that active wavefront sensing and control will be required. A low-order wavefront sensor¹ using starlight rejected by the coronagraph is essential for measuring LOS errors and differential changes in the wavefront. The low-order wavefront sensor is used for both speckle suppression and science imaging. Jitter and drift are then corrected with feedback to a Fine Steering Mirror (FSM) and to the deformable mirrors. Using the rejected starlight for wavefront control is very attractive because it is a direct measurement of the total LOS and Wavefront Error (WFE) at the coronagraph mask. It has not, however been demonstrated that wavefront sensing can achieve both the necessary bandwidth and resolution to maintain the dark hole at the 10^{-11} contrast level, even on bright host stars.

Dim stars present an additional problem for tuning the dark hole. Integration times for speckle suppression become prohibitively long because there are so few photons available. In these cases, it is assumed that the dark hole can be tuned on a bright calibration star and that the telescope can be slewed to the target star and the high-contrast field can be recovered. The success of this technique depends on finding calibration stars with similar spectral characteristics to the target star. It has not been demonstrated that this method will work in the 10^{-11} contrast regime. Furthermore, because wavefront sensors are inoperable during the slew, they may not adequately capture drift that occurs during the slew.

*joel.a.nissen@jpl.nasa.gov

Laser Metrology (MET) provides a different, complementary sensing method, one that can be used to measure changes in the alignment of the optics independent of the magnitude of the host star. In closed loop with actuators, MET actively maintains alignment of the front-end optics, thereby eliminating the dominant source of wavefront drift. Because MET is not photon starved, it can operate at high bandwidth. Furthermore, laser metrology maintains wavefront control even during attitude maneuvers such as slews between target stars. These features may significantly improve the performance and yield of future large-aperture space telescopes.

2. LASER METROLOGY

2.1 Laser gauges

Laser metrology for large coronagraph-equipped space-born observatories was first proposed for the Terrestrial Planet Finder Coronagraph². The early versions consisted of large optical benches populated with discrete optical beam splitters, retroreflectors and lenses. Recently the optical bench has been replaced by Planar Lightwave Circuit (PLC) technology, resulting in a compact lightweight beam launcher containing all the functions of the old style optical bench (figure 1a). PLC technology was developed for the optical communications industry so circuits in the communications band are easily mass produced. The principle of operation remains much the same as the original laser heterodyne interferometer system proposed for the Terrestrial Planet Finder Coronagraph. The beam launcher transmits a collimated beam through free space to a corner cube retroreflector. The reflected beam couples back into the beam launcher where it mixes with a reference beam and is coupled into a fiber optic. The current generation of MET has single-digit nm measurement error at 1 kHz sampling and single-digit nm/°C temperature coefficient. The temperature sensitivity of the PLC package is the dominant term responsible for long-term drift. For coronagraphy, it is imperative that the laser is locked to a molecular line or a temperature-controlled etalon to prevent alignment errors due to long term laser frequency drift.

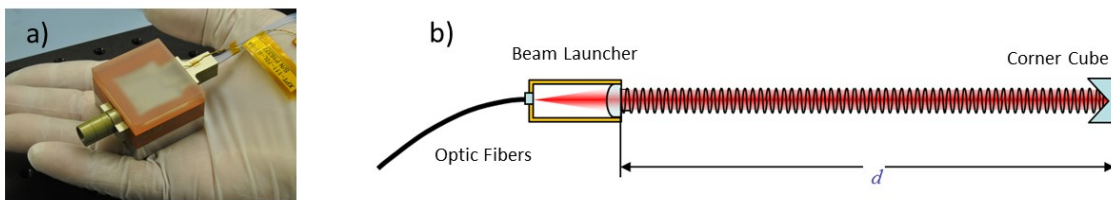


Figure 1. a) The beam launcher and optics bench are built into a small PLC suitable for mounting on lightweight-active telescope optics. b) Principle of a laser gauge. Phase modulated laser light is delivered to a beam launcher via fiber optics. The beam launcher collimates the laser light and directs it in free space to a corner cube retroreflector. The returned beam is coupled back into fiber optics and the heterodyne signal is detected with photodiodes. The metrology gauge measures displacement between the vertex of the corner cube and a fiducial surface in the beam launcher.

2.2 Optical truss

To sense alignment drift of an optic, an optical truss can be constructed to detect rigid body motion of the optic relative to a reference surface. Six gauges arranged in a hexapod are sufficient to detect displacements in all six degrees of freedom. By actuating the optic, alignment can be maintained with a feedback loop closed around the laser metrology. Figure 2 illustrates how two optical trusses can be combined to stabilize a primary and secondary mirror relative to the optic bench. In this model, the hexapods are replaced with nonapods to provide redundancy. In total, there are 18 metrology gauges used to control 12 degrees of freedom. Because each laser gauge requires only a microwatt of power, all 18 gauges can be supplied by a single 1.5-micron laser source. The geometry of the truss determines the sensitivity of the measurements to each degree of freedom. Long, narrow trusses are sensitive to tip, tilt and piston but insensitive to lateral translation and in-plane rotation of the optic.

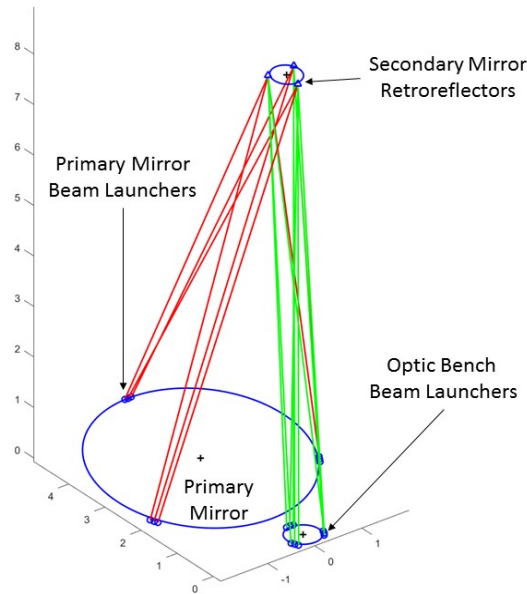


Figure 2. HabEx 4 meter $f/2.5$ unobscured aperture telescope. The primary and secondary mirrors are mounted on rigid body actuators and are actively controlled in closed loop with laser metrology. The secondary mirror motion is measured in six degrees of freedom relative to the optic bench with a laser truss (green). The primary mirror is also controlled relative to the optic bench via the primary to secondary laser truss (red) and the secondary to optic bench truss (green). A truss needs a minimum of six beams to sense six degrees of freedom. The truss in this design uses nine beams for redundancy.

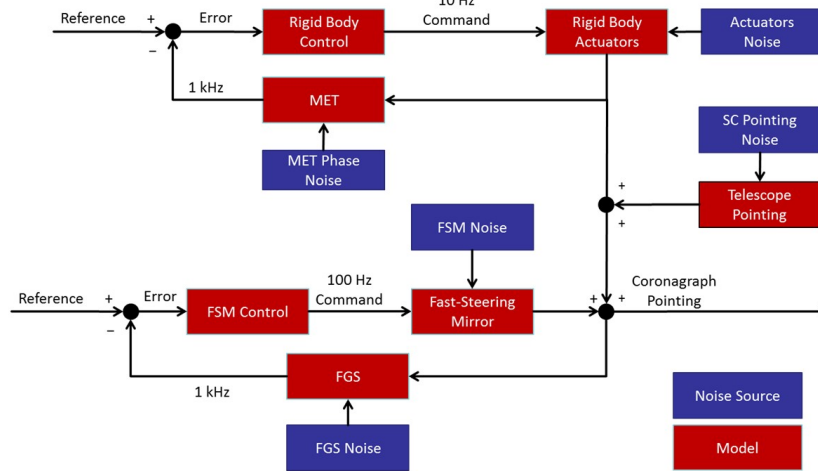


Figure 3. Because laser metrology is only sensing the alignment of the primary and secondary mirrors relative to the optic bench, MET must be supplemented by a line-of-sight control loop. A Fine Guidance Sensor (FGS) measures starlight rejected by the coronagraph to detect misalignment between the stellar image and the coronagraph mask. The line-of-sight error is then corrected with a Fine Steering Mirror (FSM) located upstream of the deformable mirrors. The LOS control loop corrects for spacecraft (SC) pointing errors as well as residual errors from the MET control loop and LOS errors from optics downstream of the tertiary mirror.

2.3 Line-of-Sight and wavefront control

In order to image a planet at the Inner Working Angle (IWA), alignment of the stellar image with the coronagraph mask is essential. LOS less than a milli-arcsecond are enough to reduce the contrast at the IWA. While thermal-induced drift can lead to LOS errors, the dominant sources of LOS will likely be jitter and spacecraft control. In these regimes, laser metrology is ineffective: either its control bandwidth is insufficient to compensate the jitter or, in the case of spacecraft pointing errors, it cannot sense the error at all. To fill the gap, MET must be supplemented with a Fine Guidance Sensor (FGS) in closed loop with a Fine Steering Mirror (FSM). The FGS can be as simple as focusing the starlight rejected by the coronagraph onto a quad cell or, preferably, a low-order wavefront sensor. Figure 3 is a block diagram of the active wavefront control. The MET control loop minimizes LOS and wavefront errors by maintaining alignment of the front-end optics. Residual LOS errors from rigid body motion of the primary and secondary mirrors along with spacecraft pointing errors are detected by the FSM.

3. MONOLITHIC PRIMARY

3.1 Residual wavefront error with closed loop MET control

In many ways, meeting performance requirements for a monolithic primary mirror is relatively easy to achieve with the metrology truss illustrated in figure 2. To assess the effectiveness of laser metrology, the HabEx baseline 4 meter unobstructed aperture was modeled. A charge six vector-vortex coronagraph was modeled and tuned to produce 10^{-10} contrast between an IWA of $3 \lambda/D$ and an outer working angle of $10 \lambda/D$, where λ is the central wavelength (550 nm) and a 10% bandwidth. Surface roughness of the front-end optics was simulated with a 2D power spectral density with 8 nm RMS WFE. Random errors were applied to the metrology gauges consistent with 0.02°C thermal control of the beam launchers, retroreflectors and interfaces. The resulting wavefront errors were fit to the first 40 Zernike coefficients according to Noll ordering. As can be seen in Figure 4, the residual wavefront error, due to rigid body motion of the primary and secondary mirror, do not generate large amplitude, high-order Zernike terms. For a monolith primary, the piston term, Z1, can be neglected and the LOS terms, Z2 and Z3 can be greatly reduced by the FGS control loop. The focus term is two orders of magnitude smaller than the MET gauge error, indicating that the high-contrast field can be maintained with 100 pm of gauge error.



Figure 4. A charge 6 vector-vortex coronagraph is insensitive to low-order Zernike terms Z1-Z8 and Z11, but is not effective in suppressing the higher order terms. The worst offenders, Z2 and Z3, line-of-sight errors, are corrected by the fine guidance control loop. For the unobscured HabEx design, high order Zernike terms, due to rigid body motion of the primary and secondary mirrors, are not produced with amplitudes large enough to affect the contrast.

3.2 Wavefront Error budget and coronagraph simulation

An error budget for HabEx metrology based on current MET capabilities is shown in figure 5. The budgeted 20°C RMS thermal control is easy to achieve for small structures such as the PLC beam launchers and the corner cubes. The contrast drift is presented in figure 6. Figure 6a is the unaberrated contrast of the charge 6 vector-vortex coronagraph. Figure 6b simulates contrast degradation due to MET gauge errors consistent with the error budget. Figure 6c, the difference between figures 6b and figure 6a, reveals that the contrast drift is an order of magnitude smaller than the unaberrated contrast even at the IWA. Planet detection would not be seriously impacted by this level of drift.

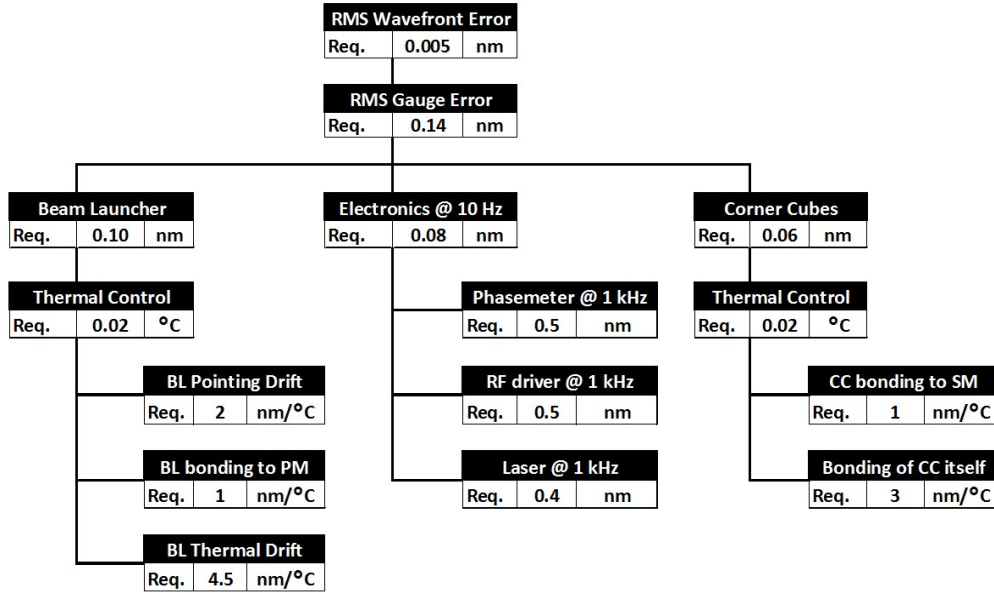


Figure 5. MET error budget for the HabEx 4 meter aperture monolithic observatory. The beam launcher, corner cube, and interface sensitivities have been demonstrated in a flight-like environment. The thermal control loop requirement is achievable due to the compact size of the MET hardware and the benign environment dictated by the necessity of thermal control for the optics in contact with the MET hardware. The phase noise is based on a simple zero-crossing phase detector.

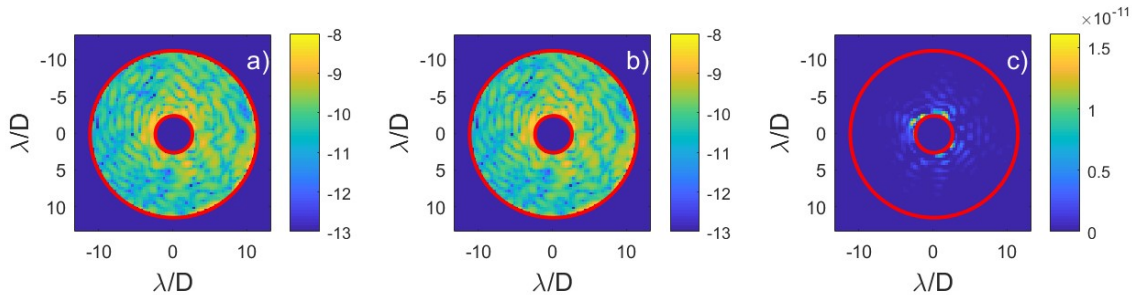


Figure 6. a) Simulation of an unaberrated HabEx coronagraph for the baseline 4 meter, unobscured monolith with a charge 6 vector-vortex coronagraph. The dark hole was tuned for 2×10^{-10} raw contrast between IWA = $2.5 \lambda/D$ and OWA = $11 \lambda/D$ (red circles). The image is displayed on a logarithmic scale. b) Simulation of the contrast with the metrology system in closed loop control with rigid body actuation of the primary and secondary mirrors. Aberrations are the result of 150 pm rms gauge drift causing rigid body motion of the primary and secondary mirrors. This level of control requires 0.020°C rms thermal control of the PLC beam launchers and the secondary-mirror mounted corner cubes. c) The difference between the unaberrated contrast and the degraded contrast due to laser metrology drift on a linear scale. The contrast drift is at least an order of magnitude smaller than the background speckle.

4. SEGMENTED PRIMARY MIRRORS

4.1 Cophasing errors

Monolithic apertures larger than 4 meters are very massive and impractical to manufacture with existing infrastructure: any large aperture space-observatory will likely have a segmented primary mirror. This presents challenges to wavefront control that are not present with a monolithic primary. In particular, a segmented primary mirror is highly sensitive to segment-to-segment dephasing and tip, tilt of individual segments. High-order Zernike terms due to rigid body motion of segments are insignificant compared to the cophasing errors.

Ground-based segmented telescopes deal with this problem with edge sensors that can measure displacements relative to neighboring segments as well as the dihedral angle between adjacent segments. While capacitive sensors have been demonstrated with sufficient resolution for coronagraphy, edge to edge sensing produces a highly coupled system prone to errors between widely separated segments. These low-order modes would have to be corrected with feedback from a low-order wavefront sensor. A laser metrology truss, on the other hand, senses motion of each segment independently and will not produce low-order modes of the primary. Figure 7 illustrates a laser metrology truss for a single segment. As noted earlier, such long, narrow trusses have poor sensitivity to lateral motion and clocking of the segment, but good sensitivity in the degrees of freedom responsible for segment cophasing.

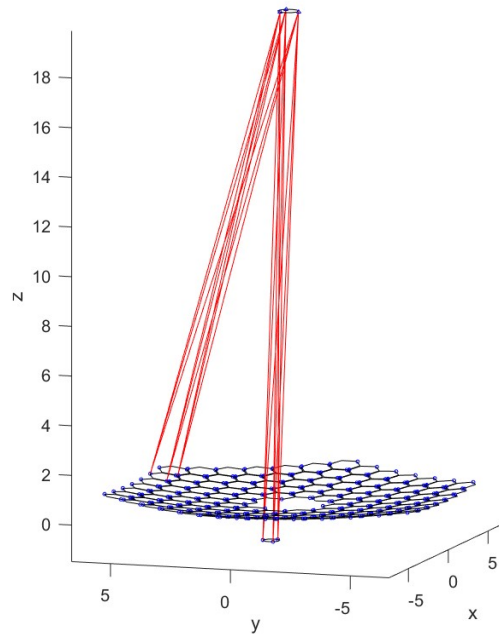


Figure 7. MET truss for the 15 meter aperture LUVOIR design. For clarity, only one MET truss for the segments is shown. This 120 segment design would require a minimum of 726 beam launchers for six degree of control for each optical element. As illustrated here, the analysis assumes nine beam launchers per segment.

4.2 MET for LUVOIR

A MET truss for a 15 meter aperture LUVOIR style telescope was analyzed in order to assess the residual wavefront error due to thermal drift. As before, secondary mirror misalignment results in global LOS errors (figure 8a.) which can be removed with the FGS. Unlike edge sensors, global LOS errors due to the primary mirror support structure are effectively controlled by the laser truss. Figure 8b presents is the same instantiation with the global tilt removed. For this

geometry, the RMS wavefront error is on average 6 times the metrology gauge error. Preliminary analysis of the LUVOIR aperture suggest that a contrast stability of 10^{-11} requires 40 pm RMS wavefront stability. As seen in the error budget in figure 9, with tight thermal control of the metrology fiducials, the LUVOIR stability requirements are consistent with current MET capabilities.

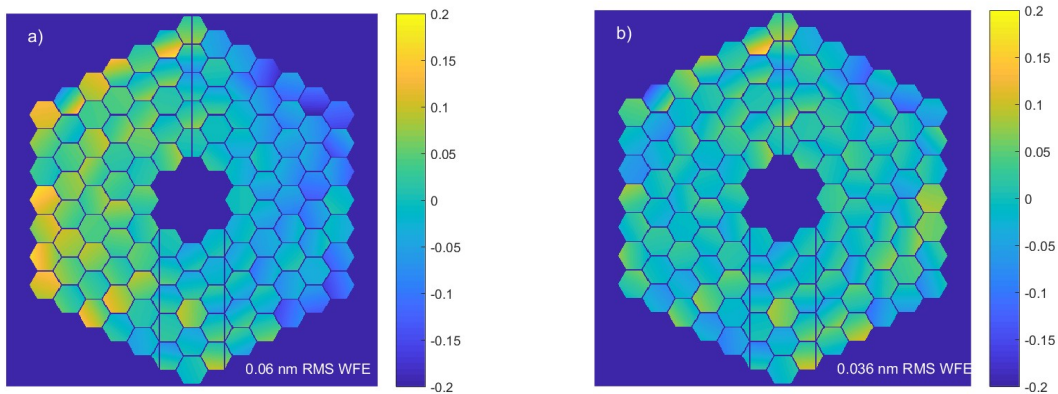


Figure 8. LUVOIR wavefront error as a function of metrology gauge error. A Monte Carlos simulation of the LUVOIR MET errors resulted in 6 pm of wavefront error per pm of laser gauge error. The simulation includes both the segmented primary and the secondary mirror. In figure 8a), misalignment of the secondary mirror introduces a line-of-sight error, here seen as a global wavefront tilt. When laser metrology is combined with a line-of-sight control around the host star, the line-of-sight error is reduced as illustrated in figure 8b). A Zernike polynomial description of the primary mirror is not helpful; a Zernike polynomial decomposition of the wavefront error due to secondary mirror misalignment is, however still relevant. In particular, MET is very effective in controlling low order Zernike terms. It is worth noting that it would take single digit μK control of low CTE carbon-fiber struts, averaged over the 20-meter strut length, to maintain the same level of secondary mirror stability.

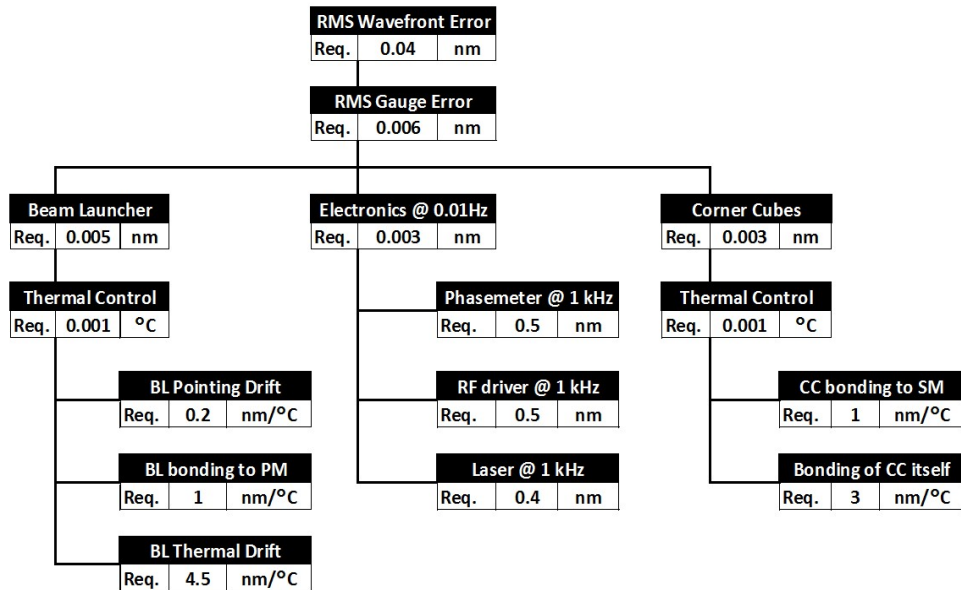


Figure 9. MET error budget for the LUVOIR 15 meter aperture segmented design. Segmented primary mirrors are very sensitive to tip, tilt and piston of individual segments. A segmented primary would need 0.001°C RMS thermal control of the beam launchers, corner cubes and interfaces.

4.3 Contrast study for a 6.5 m unobscured aperture

A 19-segment, unobscured coronagraph was also studied (figure 10). In this case, a hybrid-Lyot coronagraph with 10^{-9} raw contrast was modeled. The segments were closely packed hexagons with surface roughness modeled by a 2D power spectral density with a static 8 nm RMS WFE. The outer segments were masked to form a circular pupil. As before, a 10% bandpass centered at 550 nm was analyzed. Because the raw contrast was only 10^{-9} , the wavefront stability could be relaxed to 200 pm RMS wavefront error, which is easily achievable with current laser metrology capability.

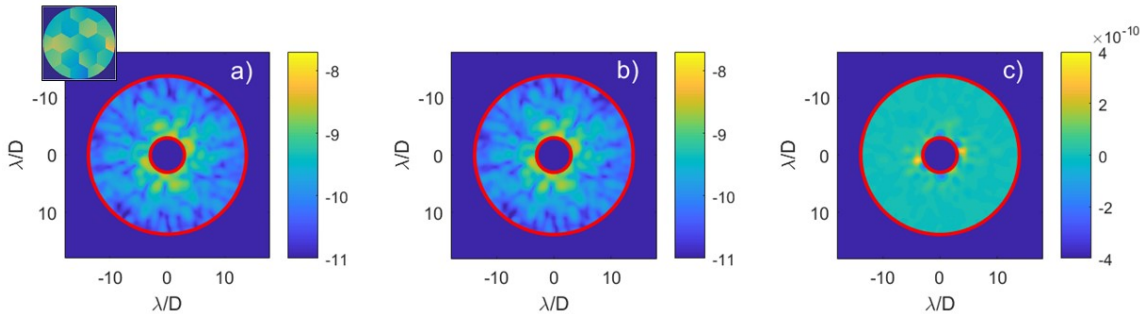


Figure 10. Simulation of two exposures from a 6.5 meter aperture, segmented unobscured telescope equipped with laser metrology. The inset is one instantiation of the aberrated wavefront due to residual segment misalignment. Figures 10a and 10b are the average intensity of 50 instantiations of the dark hole. The study simulated 50 pm rms random gauge-length errors resulting in 200 pm RMS wavefront drift. Figure 10c is the difference of figure 10a and figure 10b displayed on a linear scale. The residual drift is one to two orders of magnitude smaller than the background speckle pattern.

5. CONCLUSION

Large, coronagraph-equipped, space-borne observatories will require an unprecedented level of stability, not achievable through passive or thermal control systems; active control will be required. Wavefront sensing of starlight is an attractive method of achieving stability, but performance may be photon limited. Laser metrology is a complementary technique to wavefront sensing. By sensing alignment errors at their source, degenerate solutions for the total WFE can be resolved and corrected at their source. MET has the bandwidth, stability and resolution needed to maintain high-contrast zones for days at a time even during spacecraft maneuvers.

REFERENCES

- [1] Shi, F., Balasubramanian, K., Hein, R., Lam, R., Moore, D., Moore, J., Patterson, K., Poberezhskiy, I., Shields, J., Sidick, E., Tang, H., Truong, T., Wallace, J. K., Wang, X. and Wilson, D., "Low-order wavefront sensing and control for WFIRST-AFTA coronagraph," *J. Astron. Telesc. Instrum. Syst.* 2(1), 011021 (2016).
- [2] Shaklan, S. B., Marchen, L. F., Zhao, F., Peters, R. D., Ho, T. and Holmes, B., "Metrology system for the Terrestrial Planet Finder Coronagraph," *Proc. SPIE 5528, Space Systems Engineering and Optical Alignment Mechanisms*, 22 (September 30, 2004); doi:10.1117/12.559998.

ACKNOWLEDGEMENTS

The work described here was performed at the Jet Propulsion Laboratory, California Institute of Technology, under contract with a National Aeronautics and Space Administration.